Chemical Geology 304–305 (2012) 175–184

Contents lists available at SciVerse ScienceDirect

Chemical Geology

journal homepage: www.elsevier.com/locate/chemgeo

Research papers

Cu isotopes and concentrations during weathering of black shale of the Marcellus Formation, Huntingdon County, Pennsylvania (USA)

R. Mathur [a,*], L. Jin [b,c], V. Prush [a], J. Paul [a], C. Ebersole [a], A. Fornadel [a], J.Z. Williams [b], S. Brantley [b]

[a] Juniata College, Department of Geology
[b] The Pennsylvania State University, Earth and Environmental Systems Institute, University Park, PA 16803, United States
[c] The University of Texas at El Paso, Department of Geological Sciences, El Paso, TX 79968, United States

ARTICLE INFO

Article history:
Received 16 September 2011
Received in revised form 18 February 2012
Accepted 20 February 2012
Available online 3 March 2012

Editor: J. Fein

Keywords:
Black shale
Weathering
Cu isotopes
Marcellus shale

ABSTRACT

The complex weathering processes which govern the production of soil from bedrock have proven difficult to understand for many lithologies. Weathering of black shale is of particular interest because it releases organic carbon and heavy metals as solutes and therefore impacts the health of terrestrial and aquatic ecosystems. To understand black shale weathering, a geochemical survey was initiated for soils developed on shales of the Marcellus Formation at a zero-order catchment at a satellite site of the Susquehanna/Shale Hills Critical Zone Observatory located in Jackson Corner, Pennsylvania. This formation is an organic- and metal-rich, carbonaceous shale that underlies much of New York, Pennsylvania, Ohio and West Virginia. In this paper, we focus on the effects of weathering on variations of Cu isotopes in the shale. Cu concentration data for soil were normalized using Ti concentrations to document the mobility of Cu relative to bedrock. At both the ridgetop and valley floor, depletion profiles for Cu are documented in the soils. The Cu in the soils is depleted in ^{65}Cu (average $\delta^{65}Cu = -0.5‰ \pm 0.2$) compared to the parent material (average $\delta^{65}Cu = 0.03‰ \pm 0.15$). Consistent with loss of Cu from soils, the pore waters contain 10 ppb Cu on average and are enriched in the heavy isotope (average value $\delta^{65}Cu = 1.14‰ \pm 0.44$). Rayleigh fractionation models using the concentration and isotope data of the soils are consistent with pyrite weathering and loss of Cu from the ridgetop, but downslope transport and Cu re-precipitation at the valley floor.

1. Introduction

Earth's terrestrial ecosystems are dependent upon the uppermost portion of the lithosphere known as the soil (Amundson, 2004; Brantley et al., 2007). Few models have quantified the formation of soil satisfactorily (Ollier and Pain, 1996; Taylor and McNally, 2001; Minasny et al., 2008; Brantley and White, 2009). To enhance our understanding of this process, six Critical Zone Observatories have been established as natural laboratories. One of these, the Susquehanna/Shale Hills Observatory, SSHO, located in central Pennsylvania, is largely situated on gray shale within the Rose Hill Formation. As part of the SSHO, six other sites have also been identified to investigate weathering on shales of different composition or within different climate regimes. In this paper we focus on the satellite site located on the Marcellus black shale. Weathering of black shale is of particular interest because it releases heavy metals as solutes and can therefore impact the health of terrestrial and aquatic ecosystems.

The rock–soil interface is an ideal environment to observe Cu isotopic fractionation during rock–water interaction. Many studies (Zhu et al., 2002; Ehrlich et al., 2004; Mathur et al., 2005; Borrok et al., 2008; Pokrovsky et al., 2008; Bigalke et al., 2009; Kimball et al., 2009) have shown that biotic and abiotic reduction–oxidation reactions can result in mineral-fluid fractionations for Cu isotopes ranging from 1 to 3‰. During oxidative dissolution of copper-rich sulfides, ^{65}Cu is the favored isotopic species that has been observed to be released in the oxidized species. Given that many of the reactions occurring during weathering do not reach equilibrium, oxidative weathering can result in the fractionation of Cu isotope in different reservoirs. Examination of the Cu isotopic composition of minerals leached or enriched in Cu could potentially document the extent of the reactions that have occurred.

Copper concentrations, distributions, and speciation in soils have been reported to be a function of pedogenetic processes, anthropogenic land use factors, and the geological parent materials (Wilcke et al., 1988; Anderson et al., 2002; Beznosikov et al., 2007; Grybos, et al., 2007). For example, both texture and chemical composition of the parent material have been shown to greatly affect the accumulation and distribution of heavy metals in soils (Beznosikov et al., 2007). In one case study, soils developed on quartz-rich rock with a sandy texture showed very low concentrations of all heavy minerals including copper (Wilcke et al., 2005; Beznosikov et al., 2007). Indeed, Campbell (1976) concluded that lower copper concentrations are

* Corresponding author.
E-mail address: mathur@juniata.edu (R. Mathur).

0009-2541/$ – see front matter © 2012 Elsevier B.V. All rights reserved.
doi:10.1016/j.chemgeo.2012.02.015

found in sandy soils, coastal soils, peaty soils, and soils developed from copper-poor parent bedrock. The Cu concentrations in the Arenosols studied by Wilcke et al. (2005) contained 6.7 ppm Cu whereas the sandy soils in Beznosikov et al. (2007) contained 2.7–5.6 ppm Cu. Furthermore, higher concentrations of copper can be measured in soils derived from bedrock with greater clay and carbonate contents (Pietrzak and McPhail, 2004; Wilcke et al., 2005). Another soil type, leptosols, displayed fine textures and possessed residual metals, such as Cu, that were bound in the lime or marl that had accumulated (Wilcke et al., 2005). Most soils have an average copper concentration of 20 ppm (Anon., 1990; Kabata-Pendias and Pendias, 2001).

Humans can significantly affect the amount of copper in soils. Wilcke et al. (1998) studied how specific land uses changed soil copper concentrations: for example, arable soils had mean copper concentrations of 65 ppm with a range of 6.7–415 ppm; grassland soils yielded average copper concentrations of 36 ppm with a range of 6.7–139 ppm; forested soils showed mean copper concentrations of 74 ppm with a range of 5.5–415 ppm. The relatively high levels of copper in the arable soil could be a consequence of agrochemical applications such as animal growth stimulants, fertilizers, fungicides, bacterial sprays, and pesticides (Tiller and Merry, 1981). For example, extremely high concentrations of copper in soils have been observed at grape vineyards in Victoria, Australia where these agrochemicals containing copper have historically and frequently been applied, raising background copper concentrations of 10 ppm to levels near 250 ppm (Pietrzak and McPhail, 2004). Similarly, copper derived from fungicides caused increased copper concentration in orchard and vineyard soils in France (100–1500 ppm, Flores-Veles et al., 1996), India (29–131 ppm, Prasad et al., 1984), and Australia (11–320 ppm, Tiller and Merry, 1981).

This study aims to investigate the complex processes controlling soil production on black shales with specific emphasis on Cu leaching and its effects on Cu isotope fractionations. This will elucidate aspects of soil formation, but more importantly also will have implications for how porosity opens up and mineralogy changes in such a shale during rock-water interactions. Both processes have significant economic implications in terms of the exploitation of gas from shale. In recent years, a number of studies have focused on geochemical profiles produced by weathering processes on black shales that outcrop in other regions (Petsch et al., 2000; Jaffe et al., 2002; Tuttle and Breit, 2009; Tuttle et al., 2009). The models developed in the current paper specifically focus on copper concentrations and isotope ratios to increase our understanding of metal mobility and sulfide oxidation of the black shale. The behavior of Cu during weathering of these mineral phases is still poorly understood, but is believed to be dependent on a combination of influences such as temperature and biological sequestration (Bigalke et al., 2009, 2011). Our work builds upon several recent studies that have used Cu isotopes to study soil formation and deep weathering (Balistrieri et al., 2008; Pokrovsky et al., 2008; Bigalke et al., 2009; Mathur et al., 2010; Mirnejad et al., 2010; Bigalke et al., 2011).

2. Methods

2.1. Rock and soil sampling

Our site is a northwest-facing zero-order catchment located in Jackson Corner, Pennsylvania, vegetated largely with maple and pine forest (Fig. 1). The location lies within 12 miles of Huntingdon, PA and has presumably been logged 2–3 times since colonial times. Within the catchment, one "planar" hillslope was chosen for study — i.e., a hillslope experiencing neither significant convergent nor divergent fluid or sediment downslope transport. The hillslope, overlying black shale of the Marcellus Formation, was chosen for comparison to the soils developed on the gray and organic-poor Rose Hill shale within the Susquehanna/Shale Hills Critical Zone Observatory (SSHO) (Jin et al., 2010).

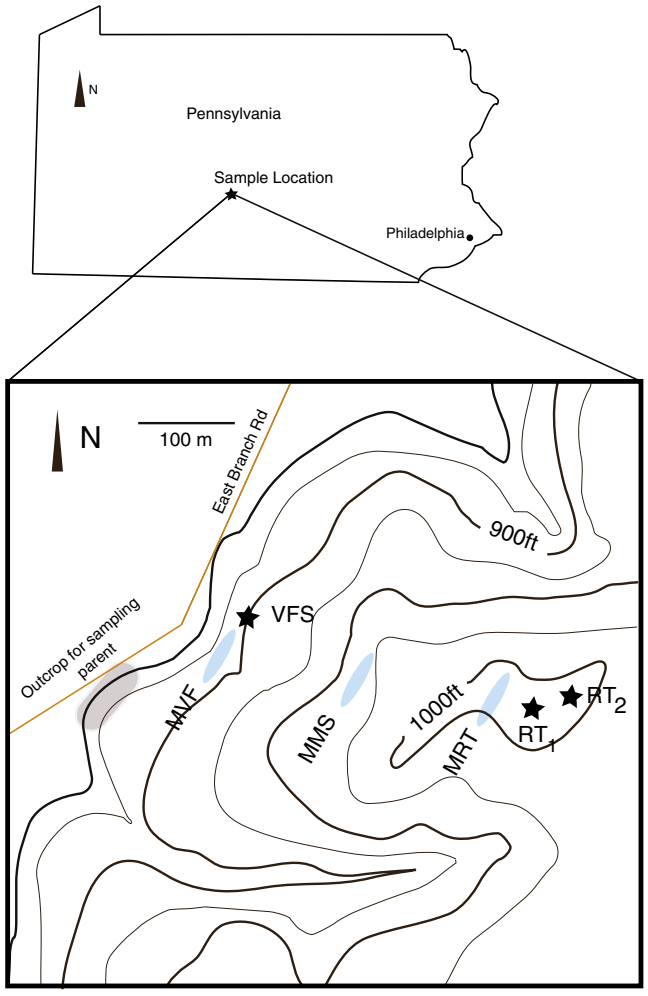

Fig. 1. Location map showing the state of Pennsylvania (USA) with the location of the soil, rock and porewater sampling. Soil locations RT_1 = Ridgetop 1, RT_2 = Ridgetop 2, VFS = Valley floor; Rock-brown colors show areas of outcropping Marcellus formation; porewater sampling locations portrayed in blue ellipses MRT = Ridgetop, MMS = middle slope, MVF = Valley floor.

The Marcellus is an easily eroded formation, and where it is present, it is therefore often found in valleys of the Appalachians. The formation is comprised of a Middle Devonian, carbonaceous black shale that forms the basal portion of the Hamilton Group, lying stratigraphically between the Seneca Member of the Onondaga Formation and the Mahantango Formation (Obermajer et al., 1997; Faill, 1998a; Soeder, 2010). The Marcellus underlies most of Pennsylvania and extends throughout the northeastern United States into Ohio, West Virginia, New York, and as far north as southeastern Canada (Obermajer et al., 1997; Faill, 1998a). The shale was deposited during one of the initial subsidence events of the Appalachian Basin during the Acadian Orogeny (Faill, 1998a; Sageman et al., 2003). Deposited during a period of rapid transgression in anoxic waters less than 100 m deep, the Marcellus Shale is characterized by its black color, high pyrite content, organic-rich nature, and lack of fossils (Sageman et al., 2003; Lash and Engelder, 2011). Depositional conditions which contributed to the organic-rich nature of the Marcellus Shale include the subtropical location of the region during Devonian times, restricted water circulation, and permanent thermohaline sea water stratification (Obermajer et al., 1997; Faill et al., 1998b).

Sampling strategies utilized at the SSHO were implemented at this satellite location. Specifically, sites were identified on ridgetops or on

planar hillslopes. These sites are referred to as 1-dimensional and 2-dimensional weathering sites respectively in that they can be interpreted in the first approximation with 1-D or 2-D models of water and sediment transport. Sites were chosen to be distant enough from roads to minimize contamination.

A total of three sites were sampled: two along the ridgetop line within 10 m of one another (RT_1, RT_2), and one at the base of the hillslope on the valley floor (VFS). One additional and similar site was also augered at Juniata College in Huntingdon, Pa and previously reported (Fornadel et al., 2008). At these sites, soils were augered by hand until refusal (Fig. 1). The depth of refusal varied from 84 cm at VFS to 83 cm at RT_2 to 134 cm at RT_1. Soil samples were collected every 5 to 15 cm, where the 0 point was defined to be the mineral soil–organic matter interface. From the three sites, a total of 35 soil samples were collected.

Seven samples of the Marcellus Shale were also collected for characterization of parent composition. Four rock fragments were collected from the bottom of the auger cores (two from VFS, one from RT_1, and one from RT_2). In addition, 2 rock fragment samples were collected from an outcrop located on the downslope side of the hillslope. This road outcrop allows sampling of shale that lies beneath the catchment (Fig. 1). One sample of the Marcellus Formation was also collected from outcrop3 nearby at the campus of Juniata College in Huntingdon, Pennsylvania. This is the same sample reported in a previous study (Liermann et al., 2011).

2.2. Porewater sampling

Porous cup tension lysimeters (soil water samplers) from Soil-Moisture Equipment Corp (model number 1900 series) were cleaned by washing with 10% nitric acid and then rinsed repeatedly with double deionized water. After cleaning, lysimeters were emplaced in three locations or "nests" located at the ridgetop (MRT, within 10 m of the augered cores for RT_1 and RT_2) and valley floor positions (MVF, within 5 m of the augered cores for VFS), as well as midway in a mid-slope position (MMS) (Fig. 1). Lysimeters were installed so as to collect pore waters from different depths spaced at 10 cm intervals. Lysimeters were emplaced in May of 2010 and the first pore waters were sampled two weeks thereafter. During the sampling period, the solute concentrations showed some variation with amount of rainfall, but no other pattern was observed that could be attributed to the perturbations due to lysimeter emplacement.

Lysimeters were placed under vacuum to −50 cbar pressure with a hand-pump one week before each collection. To sample waters, PVC tubing was lowered into the cup and water was pumped out with a syringe. Samples (30 mL) were acidified with 5 drops of ultrapure nitric acid and stored in pre-cleaned high density polyethylene (HDPE) bottles for cation analysis. The pH values of the soil water were measured with a pH meter and an electrode, which was calibrated with standard pH solutions (pH 4 and pH 7). The porous cups of these lysimeters allow only dissolved solute and particles less than 1.3 μm to be sampled. For several soil water samples, approximately half of each sample remained unfiltered while the other half was filtered further to 0.45 μm, for comparison.

2.3. Sample preparation

After collection, the sample bags were opened and covered by paper towel so that bulk soil and rock samples could air dry for a period of 72 h. Samples were then split using a riffle splitter and a portion of a representative bulk sample that included all particle sizes was ground to pass through a 100-mesh sieve (<150 μm). Approximately 6 g were set aside for elemental concentration analysis while 0.1 g were reserved for copper isotope analysis.

In order to isolate phases that could contain copper in the samples, we conducted a heavy liquid separation on powder from the Juniata College sample from outcrop 3 (Table 4). We added 11.08 g of the sample to 10 ml of a low-viscosity polytungstate fluid with specific density equal to 2.82 g/cm^3 from Geoliquids. 0.16 g of heavy mineral fraction was recovered from an 11.08 g powder for the sample from outcrop 3 at the campus of Juniata College (Table 4).

2.4. Soil elemental analysis

Soil and rock samples powdered for elemental analysis were fused with lithium metaborate and re-dissolved in 5% nitric acid. Solutions were then diluted and analyzed for elemental concentrations using inductively coupled plasma atomic emission spectrometry (ICP-AES) on a Perkin-Elmer Optima 5300 at the Pennsylvania State University.

Elemental concentrations of Cu were normalized to infer enrichment or depletion throughout the soil profile relative to elemental concentrations in the parent rock material using the mass transfer coefficient τ (Brimhall and Dietrich, 1987):

$$\tau_{i,j} = \frac{C_{j,w} \times C_{i,p}}{C_{j,p} \times C_{j,p}} - 1 \quad (1)$$

Here C refers to concentrations of immobile or mobile elements (i, j, respectively) in parent (p) or weathered material (w). Ti was used as the immobile element (i), because plots of τ calculated using different immobile elements consistently documented that Ti was the most immobile element. Parent values were calculated as the average of 7 different samples; 4 from the deepest soil samples collected from the auger cores, 3 from the outcrop of the Marcellus Shale located near the site. All of the compositions for the 7 parent samples are listed in Table 4, including average Cu values and uncertainties presented as ±1 standard deviation (±1σ). Errors in the τ calculation were computed using error propagation as outlined previously (Jin et al., 2010), where most of the uncertainty in τ is due to variability in the parent composition ($C_{Ti,p}$ and $C_{Cu,p}$). The relative errors in soil composition measurements are from analytical uncertainties (5% for $C_{Ti,w}$ and 10% for $C_{Cu,w}$).

2.5. X-ray diffraction and SEM analysis

X-ray diffraction analysis (XRD) was used to determine the major mineral phases present in one parent rock sample (outcrop 3 from Juniata College) and the heavy mineral separate taken from that sample of outcrop 3. The rock and the mineral separate were powdered to <75 μm and side-packed to a sample holder to avoid preferential orientation of the clay minerals (Moore and Reynolds, 1997). The analyses were performed on a Scintag X-ray diffractometer, and were scanned from 2 to 80° 2Θ using a step of 0.02° at a rate of 2.50°/min. After background data were subtracted out, individual peaks and mineral phases were identified.

The heavy mineral aliquot and 2 soils from the base of the RT_1 augered core were also epoxy-mounted for analysis on a scanning electron microscope (SEM) using energy dispersive x-ray spectroscopy (EDS). SEM images were made using a JEOL 6460 at 20Kev with EDS chemical data measured using Cu as a standard. Patterns were interpreted using INCA software by Cambridge.

2.6. Water chemistry analyses

Acidified pore water samples were analyzed for major cation concentrations using the ICP-AES and for trace element concentrations including Cu using a quadrupole ionized coupled plasma mass spectrometer (ICP-MS) at the Pennsylvania State University. The precision is estimated to be better than ±3% for major elements and ±10% for minor elements.

2.7. Copper isotope analysis

For isotopic analysis, all water samples were purified with ion exchange chromatography (IEC). Gravimetric checks were conducted on all samples to ensure >94% yields for all reported values. The yield measurements were accomplished by withdrawing approximately a 0.1 g mass aliquot for pre- and post-column chromatography for Cu concentration analyses. We modified the IEC procedures from the literature (Marechal et al., 1999; Marechal and Albarede, 2002; Mathur et al., 2005, 2009) depending on the solution matrix as outlined below.

For the soils and rocks, 0.1 g of powdered material were dissolved by ultrapure hydrofluoric acid in heated (120 °C) Teflon beakers for 24 h. The beakers were uncapped and the solutions dried on a hotplate at 80 °C overnight. The salts were further dissolved in ultrapure aqua regia and allowed to dry on a hot plate at approximately 100 °C. The salts were then processed with a modified ion exchange column chemistry procedure by Marechal et al. (1999) described below. Specifically, 10 ml Bio-Rad chromatography columns were filled with 3 mL of AG MP-1 anion exchange resin. After we allowed resin to settle and we removed any bubbles, the resin was cleaned by filling the columns with 18.2 Ω Milli-Q and 0.5 N nitric acid. The resin was then allowed to drain completely. 7 mL of 8 N HCl were added and allowed to pass through the columns, followed by 1 mL of the prepared sample solution. 17 mL of 8 N HCl were eluted and discarded and the next 32 mL were collected. The 32 mL were allowed to dry overnight on hotplates at approximately 80–100 °C. After the samples had dried, the same protocol was repeated to insure that all unwanted elements had been removed.

For the pore water, we dried down a sufficient amount of solution to obtain 200 ng of Cu for isotopic analysis. On average, we dried down 20 ml of solution overnight in a Teflon beaker on a hot plate at 60°. Since the total concentration of ions did not exceed the ability of 1.8 ml of AG-MP1 resin to separate Cu from the other ions, we used the protocol from (Marechal et al., 1999).

After column separation chemistry had been completed, the samples were diluted with ultrapure 2% HNO_3 and readied for injection into the Multi-Collector ICPMS (MC ICPMS). Samples were diluted to 200 ppb and injected into the MC-ICPMS, the Micromass Isoprobe at the University of Arizona, using a microconcentric nebulizer. The concentration generated between 1.5 and 3 V in low resolution mode. Background ^{63}Cu and ^{65}Cu ranged from 0.0005 to 0.001 V and on-peak backgrounds were subtracted out of each measurement. In order to correct for instrumentation mass bias standard-sample-standard bracketing was employed. The authors did not find any increase in precision or accuracy with the addition of Zn or Ni standards to correct for mass bias.

The Cu isotope ratios are reported in conventional per mil notation against the NIST 976 standard:

$$\delta^{65}Cu = \left(\frac{R_{sample}}{R_{standard}} - 1\right) \times 1000 \quad (2)$$

Here R is defined as the $^{65}Cu/^{63}Cu$ ratio. Each solution was measured in triplicate with a 40 ratio method. Thus, the reported ratios are an average of 120 ratios. To assess errors, we monitored the variation of the NIST 976 throughout each of five 4-day sessions. The 2-σ variation of the standard over the 20 day interval was observed to equal 0.14 per mil. Given that the standard was the most analyzed sample, we assume this to be the error for the samples. The triplicate sample solution measurements all fell within the reported error. Further analytical procedures are described in Mathur et al. (2005, 2009).

3. Results

3.1. Soil, rock and pore water chemistry

The concentrations of Cu in parent rocks and soils vary from 10 to 70 ppm and show no consistent trend with depth (Tables 1–4). The concentrations of Cu in Marcellus shale rock are slightly higher than crustal averages (McLennan et al., 2006), but not as high as observed in other black shale units of equivalent age (Tuttle et al., 2009). The Cu concentration in the heavy mineral split separated from the outcrop 3 sample is almost 2 orders of magnitude higher (674 ppm) than that measured in the soils and parent rocks. Therefore a significant fraction of the Cu was contained in a heavy mineral of density ≥ 2.82 g cm^{-3} such as pyrite (density = 5.0 g cm^{-3}). This split represented 1.4 wt.% of the outcrop 3 sample, which itself contained 18 ppm Cu (Liermann et al., 2011). If all of the copper in the Marcellus outcrop 3 sample were derived from pyrite in the heavy mineral separate, then the calculated Cu concentration (1.4% × 674 ppm Cu) in that sample would be 9.7 ppm. Therefore, at least half of the Cu in the outcrop 3 sample, and thus in Marcellus shale, resides in a heavy mineral such as pyrite and the rest is present in the less dense minerals such as clays.

In Fig. 2, depth profiles for $\tau_{Ti,Cu}$ are plotted for each location (RT_1, RT_2, VFS). To calculate $\tau_{Ti,Cu}$, the parent concentration of Cu ($C_{j,p}$) was set equal to the average concentration of Cu from seven rock fragments collected as the bottom-most sample from each augered hole and outcrops. For each hole, the rock fragment was recovered at the depth of refusal, shown on the plots as the dashed horizontal line. In every case, the value of the copper concentration in the rock sample from the base of the hole lies within ±2σ of the measured copper concentrations in the averaged Marcellus shale reported here (Table 4).

Nearly all the values of $\tau_{Ti,Cu}$ for soil samples above the depth of refusal are negative, consistent with loss of Cu from the soil relative to the parent. In each core, one or two samples at various depths do not show depletion of Cu, perhaps due to heterogeneity of the parent composition.

The pH values of soil pore waters range from 3 to 5 and do not show variation with depth (Table 5). It must be noted of course that these measured pH values do not represent the in situ soil water pH values because of the likelihood of CO_2 degassing while the water is in the lysimeter. The concentrations of dissolved Cu measured (Table 5) in pore waters varied from 0.7 to 13 ppb. Filtered and unfiltered pore waters from the same lysimeter have almost the same concentrations of Cu. Fig. 3 displays the depth variations of copper concentration in the pore waters collected over two months. The maximum dissolved Cu concentrations are higher in the shallow lysimeters than at depth (Fig. 3). Furthermore, elevated concentrations

Table 1
The Cu concentration, isotope, and mass balance coefficient data at ridge top (RT_1) site.

Sample number	Depth[1] (cm)	Cu (ppm)	δ^{65}Cu (‰)	τ_{Cu}
RT_1-1	10	25	−1.04	−0.62
RT_1-2	20	30	−0.86	−0.54
RT_1-3	30	15	−0.76	−0.77
RT_1-4	40	25	−0.66	−0.59
RT_1-5	50	20	−0.62	−0.67
RT_1-6	60	25	−0.51	−0.60
RT_1-7	70	65	−0.51	0.09
RT_1-8	80	25	−0.51	−0.61
RT_1-9	90	10	−0.64	−0.84
RT_1-10	100	40	−0.56	−0.36
RT_1-11	110	10	−0.32	−0.84
RT_1-12	120	10	−0.46	−0.84
RT_1-13	130	35	−0.58	−0.45
RT_1-14	140	10	−0.39	−0.84

[1] Mid-range depth of the sampled interval.

Table 2
The Cu concentration, isotope, and mass balance coefficient data at ridge top (RT_2) site.

Sample number	Depth[1] (cm)	Cu (ppm)	δ^{65}Cu(‰)	τ_{Cu}
RT_2-1	0	70	n.a.	0.07
RT_2-2	17	40	0.06	−0.39
RT_2-3	27	35	−0.68	−0.47
RT_2-4	38	40	−0.37	−0.34
RT_2-5	50	35	−0.35	−0.43
RT_2-6	68	40	−0.36	−0.36
RT_2-7	83	55	−0.25	−0.08

[1] Mid-range depth of the sampled interval.

of Cu are consistently found in the ridgetop (MRT) and midslope (MMS) lysimeters regardless of the sampling date.

3.2. Rock and heavy mineral mineralogy

XRD patterns from the parent sample (outcrop 3) reveal the presence of illite (~40 wt.%), montmorillonite (<10 wt.%), quartz (~40 wt.%), plagioclase (4 wt.%), and pyrite (2 wt.%). Other minerals such as rutile were present in trace levels at <2 wt.%. SEM EDS analysis revealed occasional grains of relatively high density that contained Fe and S, consistent with the mineral pyrite (see also Liermann et al., 2011).The diffraction pattern of the heavy mineral separate from the outcrop 3 sample revealed only the presence of pyrite and rutile.

3.3. Copper isotopes of soils, rocks and soil waters

The copper isotopic compositions of the outcrop, the heavy mineral separate from the outcrop rock, and rocks from augered cores are 0.04 ± 0.16‰ (1σ, $n = 8$). This value is within the range observed for average continental crust (Li et al., 2009). In contrast, the soils are more isotopically depleted than the parent (average $\delta^{65}Cu = -0.5 \pm 0.2$‰). Furthermore, they display two different patterns in the Cu isotopic composition with depth (Fig. 4). For both ridgetop sites, shallow soils are isotopically depleted in ^{65}Cu but approach parent values deeper in the profile. The pattern of Cu isotopic signature from depleted at the surface back to parent values at depth is identical to the pattern of ^{65}Cu isotopes that were previously reported (Mathur et al., 2009, 2010) in deeply weathered leach cap rocks overlying porphyry copper deposits. In contrast to the two ridgetop soils, the δ^{65}Cu signature in the valley floor soils remained almost constant throughout the profile.

All but 2 of the pore waters analyzed here have enriched Cu isotopic signatures in comparison to the soils and rocks (0.7–1.7‰). No relationship is observed between Cu concentrations and pH or Cu isotope ratios (Table 5). The slightly positive Cu isotopic compositions of the pore waters are similar to acid mine drainage waters as well as river and ocean waters as reported in the literature (Vance et al., 2008; Kimball et al., 2009).

Table 3
The Cu concentration, isotope, and mass balance coefficient data at valley floor (VFS) site.

Sample number	Depth[1] (cm)	Cu (ppm)	δ^{65}Cu (‰)	τ_{Cu}
VFS-1	10	14	−0.57	−0.55
VFS-2	15	56	−0.47	−0.52
VFS-3	20	11	−0.43	−0.45
VFS-4	30	70	−0.47	−0.30
VFS-5	35	30	−0.54	−0.23
VFS-6	40	31	−0.60	−0.24
VFS-7	45	36	−0.46	−0.21
VFS-8	52	44	−0.54	−0.19
VFS-9	57	37	−0.53	−0.15
VFS-10	62	53	−0.36	−0.11
VFS-11	67	37	−0.41	−0.09
VFS-12	72	41	−0.37	−0.05
VFS-13	77	38	−0.36	0.01
VFS-14	82	34	−0.58	0.04

[1] Mid-range depth of the sampled interval.

Table 4
The Cu concentration and isotope data of the parent rock samples.

Sample	Description	Cu (ppm)	δ^{65}Cu (‰)
RT_1	Rock fragment at bottom of core	10	−0.09
RT_2	Rock fragment at bottom of core	55	0.25
VFS 1*	Rock fragment at bottom of core	48	0.00
VFS 2*	Rock fragment at bottom of core	39	−0.17
Outcrop 1	Fresh rock from outcrop at base of slope	124	0.02
Outcrop 2	Fresh rock from outcrop at base of slope	130	NA
Outcrop 3	Fresh rock from outcrop near Juniata College	18	0.02
Parent	Average ± 1 standard deviation	60 ± 48 (n = 7)	0.05 ± 0.14 (n = 6)
Outcrop 3 HL	Heavy liquid separate, outcrop 1	674	0.21

NA = not available, *separate rock chips taken from the bottom of the augered hole.

4. Discussion

4.1. Location of Cu in Marcellus shale

An analysis of all 7 parent samples (Table 4) yields an average copper concentration of 60 ± 48 ppm (1σ), a value that is greater than average crustal abundance (28 ppm) (Taylor and McLennan, 1985). The values lie within the range of Cu concentrations found in a similar geologic unit of the same age reported previously (Tuttle et al., 2009). The large range might be explained by the presence of Cu-rich phases such as chalcopyrite, $CuFeS_2$, or Cu-containing pyrite, FeS_2, that vary in abundance in the parent. Consistent with this, the Cu concentration in the heavy mineral fraction is much higher, at 674 ppm (Table 4). Thus, one or more dense phases contain Cu in the Marcellus. XRD of the heavy fraction identified only pyrite and rutile; furthermore, neither XRD nor SEM EDS identified chalcopyrite nor any other Cu-rich sulfide mineral.

Given these observations, we conclude that much of the Cu in the parent shale resides in pyrite. Specifically, the total concentration of Cu in the sample used for heavy mineral separation is 18 ppm (Liermann et al., 2011). Pyrite in that outcrop 3 sample was previously estimated to be present at concentrations of ~2 wt.% based on quantitative XRD and bulk elemental analysis (Liermann et al., 2011). Liermann et al. (2011) also report approximately1.0 wt.% S. As measured in the heavy mineral separate, 9.7 ppm of the Cu resides within the pyrite. Thus, approximately half of the Cu present in the Marcellus shale is attributed to pyrite. The remaining Cu is attributed to organic matter or the silicate fraction (likely clays) in the parent.

4.2. Cu depletion in soil

All the $\tau_{Ti,Cu}$ plots constitute depletion profiles (Brantley and White, 2009). Maximum Cu loss observed in an individual layer was calculated to equal 84%, 47% and 55% in RT_1, RT_2, and VFS respectively (Fig. 2, Tables 1–3). The $\tau_{Ti,Cu}$ plots are therefore consistent with loss of up to 50–80% of the Cu in upper layers either as solutes or particles due to weathering of the Cu-containing pyrite, organic matter, or Cu-containing silicates. Mobilization of Cu in dissolved or colloidal form from soils has been observed in other sites (Keller and Domergue, 1996; de Jonge et al., 2004).

The depth of refusal of augering is the point where a hand auger can no longer penetrate. Particles formed at the ridgetop at this depth by fracturing and disaggregation of bedrock are weathered throughout their upward path as they move up vertically through the regolith until they are eroded away from the surface. Thus, at the RT_1 and RT_2 ridgetop sites, material has largely eroded at the

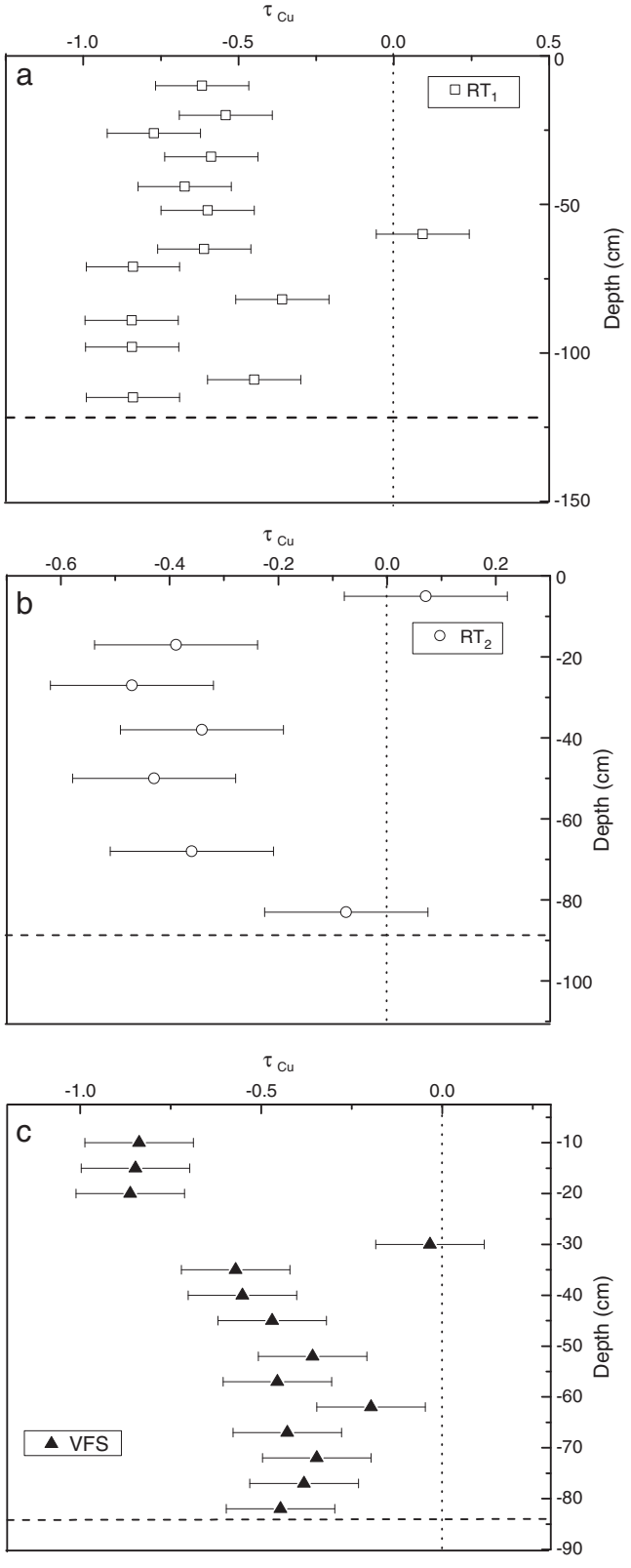

Fig. 2. $\tau_{Ti,Cu}$ versus depth for three locations: a) RT_1, b) RT_2, c) VFS. Horizontal dashed line indicates depth to refusal for each augered hole. Error bars represent uncertainties in calculated $\tau_{Ti,Cu}$, estimated from error propagation following Jin et al. (2010).

land surface while the weathering interface with unaltered rock has advanced downward. For such a 1-D upward-transport model of rock particles with ongoing downward flow of porefluids that leach Cu out of the particles, we would have expected increasingly negative

Table 5
Pore water Cu concentration and isotope data.

Name	Date	Location	pH	Depth (cm)	δ^{65}Cu (‰)	Cu (ppb)
JP10012	5/14/2010	MMS	3.86	20	1.36	11.4
JP10034	5/21/2010	MMS	3.77	20	1.37	15.0
JP10036	5/21/2010	MMS	3.74	30	−0.02	6.0
JP10035	5/21/2010	MMS	4.36	100	1.20	5.0
JP10056	5/28/2010	MMS	3.85	20	0.96	12.0
JP10057	5/28/2010	MMS	5.26	100	1.31	13.0
JP10058	5/28/2010	MMS	3.85	30	1.40	4.0
EB10020	6/23/2010	MRT	4.28	40	1.41	7.0
JP10019	6/23/2010	MRT	4.58	40	1.73	12.0
JP10041	6/23/2010	MRT	4.31	40	0.77	10.6
JP10042	6/23/2010	MRT	4.19	30	0.85	3.9
JP10043	6/23/2010	MRT	4.63	20	1.36	4.1
JP10063	6/23/2010	MRT	4.35	40	1.14	10.0
EB10002	6/23/2010	MVF	NA	20	NA	4.1
EB10006	6/23/2010	MVF	3.87	80	NA	0.7
JP10001	6/23/2010	MVF	4.19	10	NA	2.1
JP10002	6/23/2010	MVF	4.22	20	NA	2.3
JP10003	6/23/2010	MVF	4.22	30	NA	1.0
JP10004	6/23/2010	MVF	4.46	50	NA	1.0
JP10005	5/14/2010	MVF	4.49	80	NA	0.8
JP10006	5/14/2010	MVF	4.08	40	NA	1.3
JP10022	5/14/2010	MVF	3.7	10	NA	2.6
JP10023	5/14/2010	MVF	3.85	20	NA	2.0
JP10024	5/14/2010	MVF	3.97	30	NA	1.3
JP10025	5/14/2010	MVF	5.34	60	NA	1.9
JP10026	5/14/2010	MVF	4.41	50	NA	0.8
JP10027	5/14/2010	MVF	4.4	80	NA	1.4
JP10028	5/14/2010	MVF	4.03	40	NA	2.0
JP10045	5/28/2010	MVF	3.77	10	NA	2.4
JP10046	5/28/2010	MVF	3.83	20	NA	2.1
JP10047	5/28/2010	MVF	3.99	30	NA	1.2
JP10048	5/28/2010	MVF	4.26	50	NA	0.9
JP10049	5/28/2010	MVF	4.36	80	NA	0.8
JP10050	5/28/2010	MVF	4.01	40	NA	1.3

NA = not available.

$\tau_{Ti,Cu}$ values in the soil samples from the upper portions of the cores where duration of weathering is effectively longer. In contrast, for both RT_1 and RT_2, the values of $\tau_{Ti,Cu}$ do not show a smooth trend upward but rather show loss of Cu immediately at the parent–soil interface, and then more or less constant values upward. Furthermore, Cu concentrations in pore fluids are variable, but generally higher at the surface than at depth.

We consider three alternative explanations for the relative constancy in $\tau_{Ti,Cu}$ versus depth and the trends in dissolved Cu concentrations:

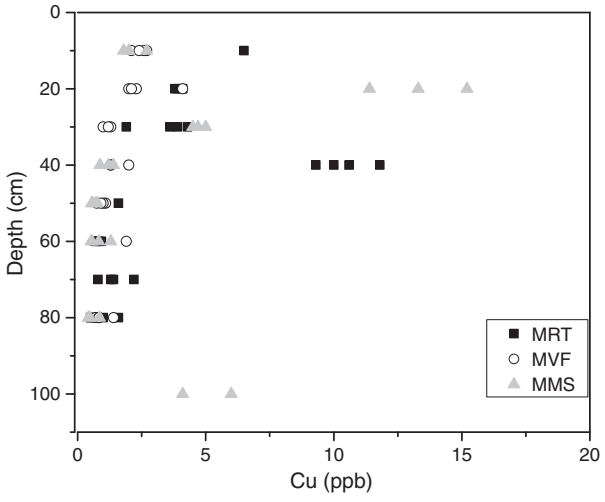

Fig. 3. Cu concentration (ppb) measured in pore waters plotted versus depth for lysimeters at the ridgetop (MRT), valley floor (MVF), and midslope (MMS).

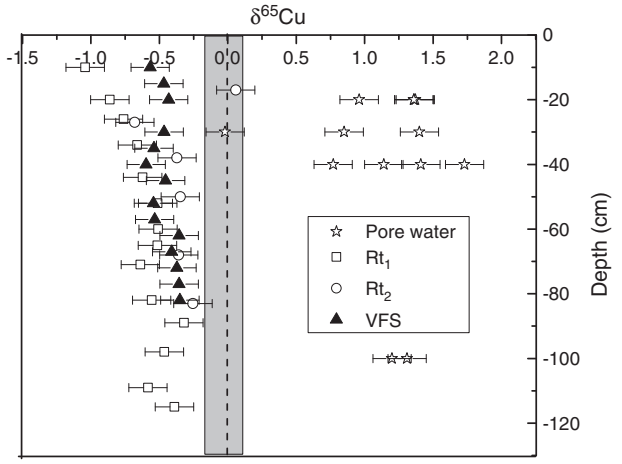

Fig. 4. Cu isotope compositions of samples of soil (from ridgetop sites RT_1, RT_2, and valley floor site VFS), parent rocks (gray bar, this was calculated as the average of the Cu isotope measurements from parent materials n = 7), and pore waters (lysimeter samples).

i) the soil is highly mixed — for example by bioturbation — such that the expected trend from 0% Cu loss at depth to significant depletion at the surface has been homogenized over much of the soil depth; ii) the most reactive of several Cu-containing phases (presumably pyrite) becomes completely depleted upon formation of soil from bedrock at the same time that aqueous Cu is biocycled upward, explaining high aqueous Cu concentrations in porefluids; iii) pyrite oxidation and organic matter decomposition occur at the bedrock–soil interface but in addition, Cu leached from the less reactive Cu-containing phases in upper soil layers is transported downward and re-precipitated or adsorbed in lower layers.

The first alternative is unlikely as the dominant explanation because soil mixing has been reported to be relatively slow in soils in the northeastern USA. (Kaste et al., 2007). Furthermore, such mixing is largely inconsistent with the relatively high $\tau_{Ti,Cu}$ values at some depths in the RT_1 profile — in other words, such high values at some depths (i.e., at 60 cm in RT_1 and the surface of RT_2) obviously have not been homogenized by mixing (Fig. 2). Finally, mixing generally affects profiles more in the upper tens of centimeters than at depth and is therefore not likely to explain constant $\tau_{Ti,Cu}$ over the entire RT profiles. Alternatives (ii) and (iii) are considered in the next paragraphs.

The relatively constant $\tau_{Ti,Cu}$ — depth plots could be consistent with pyrite oxidation and Cu loss that completely leaches the Cu from the pyrite as soon as particles cross the interface defined by the point where bedrock disaggregates into particles that can be augered. Specifically, since approximately half the Cu was inferred to be in pyrite, 100% loss of pyrite at the point of augering refusal would be consistent with 50% loss of Cu. It is well known, for example, that under surficial conditions, metal sulfides rapidly oxidize to release protons and mobilize metals such as Cu to pore water (Du Laing et al., 2007). Furthermore, in laboratory experiments with sulfide-containing rocks, fast oxidation and loss of Cu is observed under relatively oxidizing conditions (Neaman et al., 2005a, 2005b). Neaman et al. (2005a) concluded that mobilization of Cu was especially enhanced when organic ligands were present under oxic conditions because Cu forms strong complexes with chelating ligands. The high organic content of the Marcellus is therefore consistent with rapid oxidative loss of Cu.

Some of the porewater data is consistent with this hypothesis. For example, Cu may have been released from deep in the soil at midslope because Cu concentrations were observed to be high in a few lysimeter samples taken from that location at 100 cm depth (Fig. 3). Furthermore, such high concentrations at the bedrock–soil interface of the midslope soil may advect in porefluids down the hillslope during transient perched water tables after large rain events. Such downslope transport at the Rose Hill shale bedrock–soil interface has also been observed in the Shale Hills Critical Zone Observatory about 20 miles to the northeast (Jin et al., 2010, 2011). Cu tends to remain soluble at low pH values such as those observed in the Marcellus soil porewaters. This low pH in soils is due both to acid rain from coal-burning to the west but also may reflect acid generated due to pyrite oxidation (Nordstrom, 1982).

Oxidative release of Cu at the bedrock–regolith interface is not, however, consistent with the observation that Cu is found in porewaters even at very shallow depths or that Cu is sometimes elevated in concentrations at the surface and at rooting depths of 20–40 cm (Fig. 3). If all the Cu in pyrite is removed at depth, leaving a relatively insoluble Cu-containing clay or organic phase, then high-Cu concentrations in porewater should not occur at the surface. However, according to scenario (ii), Cu may be solubilized at depth, taken up by roots into biomass, and later recycled back to the soil when leaves drop and are decomposed. Such biocycling is known to happen for nutrients and for elements such as Cu that form strong organic complexes (Bigalke et al., 2010; Brantley et al., 2011). Upward biocycled Cu can then be concentrated by evapotranspiration losses of H_2O at the surface or at rooting depths.

The third explanation for the Cu profiles also relies on complete oxidative leaching of Cu at the bedrock–soil interface as well as evapotranspiration-driven concentration of porefluids, but, instead of biocycling invokes leaching of Cu from the remaining Cu-containing clay or organic matter found higher in the profiles. According to this explanation, the large range in Cu concentrations in porewaters — from 1 to 16 ppb (average: 9 ± 4 ppb; Table 5) — reflects both evapotranspiration and Cu mobilization during leaching.

Either scenario (ii) or (iii) could also be accompanied by sorption or precipitation of Cu out of porefluids at depth. Indeed, the behavior of heavy metals and their bioavailability in soils is very much affected by the processes of adsorption and precipitation (Gimeno-Garcia et al., 1995). In most soil solutions, for example, copper mostly exists as Cu^{2+} with minor proportions of Cu^{+} (Weber et al., 2009). As described by Bigalke et al. (2010), Cu often adsorbs onto negatively charged clay minerals or is incorporated into Fe oxides during precipitation. Cu also commonly complexes with soil organic matter (Bigalke et al., 2010).

The lack of correlation between Cu and pH (Table 4) is inconsistent with precipitation driven by pH changes. In contrast, the higher aqueous Cu concentrations observed in the upper layers compared to the deeper layers could be consistent with organic ligand-promoted leaching of Cu at the surface and Cu precipitation at depth as the organic ligands are decomposed by heterotrophic soil bacteria.

Overall, then, soil profiles are consistent with oxidative weathering of Cu-containing pyrite near the bedrock–soil interface accompanied either by i) upward Cu biocycling, or ii) organic-promoted Cu leaching from other phases higher in the profile. In either case, lateral flow out of the ridgetop and middle slope profiles along the bedrock–soil interface or along shallower horizons most likely carries high-Cu porewaters into the middle slope and the valley floor sites intermittently. Precipitation or sorption of Cu could be occurring as organic ligands decompose. Based on the elemental chemistry measurements, we cannot distinguish which scenario, (ii) or (iii) is most likely for the soils. However, based on Cu isotope evidence cited below, we will show that scenario (iii) with precipitation of Cu downslope or at depth is the most likely explanation of all the data.

4.3. Cu isotopes

In general, the isotopic composition of the soil material is isotopically depleted in ^{65}Cu compared to the parent material while the porewaters are enriched. Consistent with these observations, many

studies (Zhu et al., 2002; Mathur et al., 2005; Markl et al., 2006; Kimball et al., 2009; Mathur et al., 2010; Palacios et al., 2011; Wall et al., 2011) have demonstrated that oxidation of Cu-containing sulfides preferentially releases ^{65}Cu to solution and thus preferential retains ^{63}Cu in residual material. Thus, in general, the isotopically depleted Cu values in the soils are consistent with the inferred mechanism of oxidative weathering of pyrite.

Except for the uppermost samples from VFS which are not as depleted as those in RT_1 and RT_2, most of the data for Cu isotopes in soil are similar in that they show more depleted values in the surface compared to depth (Fig. 4). The geochemical models developed below demonstrate how this observation can be explained.

Cu sorption, precipitation, complexion with organic matter, and uptake into plants could all potentially impact the copper isotopic composition. For example, adsorption of Cu onto Fe-oxides has been shown to generate a fractionation described by $\Delta^{65}Cu_{(solid\text{-}solution)} = \delta^{65}Cu_{solid} - \delta^{65}Cu_{solution} = 1‰$ (Balistrieri et al., 2008; Pokrovsky et al., 2008). This process alone cannot explain the isotopic depletion seen in the residual soils however because it predicts that the soils should show isotopic enrichment with depth or downslope and this was not observed (Fig. 4). For example, the contaminated soils analyzed by Bigalke et al. (2010) displayed an isotopic enrichment with depth that was attributed to sorption. Likewise, plants are likely to preferentially incorporate the lighter ^{63}Cu isotope (Pokrovsky et al., 2008; Bigalke et al., 2009; Weinstein et al., 2011) which can only explain the upper portion of RT_2. Again however, such a mechanism cannot explain the isotopically depleted soils observed here. This latter observation leads us to infer that biocycling of Cu upwards and into biomass (scenario ii) is not a likely mechanism to explain the Cu isotopic data.

However, Mathur et al. (2005), Borrok et al. (2008) and Kimball et al. (2009) all demonstrated that oxidative leaching of sulfides under abiotic conditions releases isotopically enriched ^{65}Cu into solution, as observed in the Marcellus porewaters (Fig. 5). Mathur et al. (2005) and Kimball et al. (2009) also demonstrated that bacteria that oxidize S or Fe at pH<2 can cause oxidation of Cu in Cu-containing sulfides, releasing Cu that is isotopically enriched in ^{65}Cu, similar to Cu in porewaters in the Marcellus soils. Such biotic effects may also be occurring in the Marcellus soils. However, they may not be as important in the Marcellus since pH values of porefluids are not near pH 2 (and most likely were not near 2 even before CO_2 degassing). Furthermore, Mathur et al. (2005) also argued that the bacteria preferentially incorporated ^{65}Cu. No such substantive incorporation in bacteria or soil organic matter is indicated in the bulk Marcellus soils where Cu isotopic depletion instead of enrichment is observed in 31 of 34 measurements, at all depths (Fig. 4). Thus, once again, we see no Cu isotopic evidence to support significant Cu biocycling.

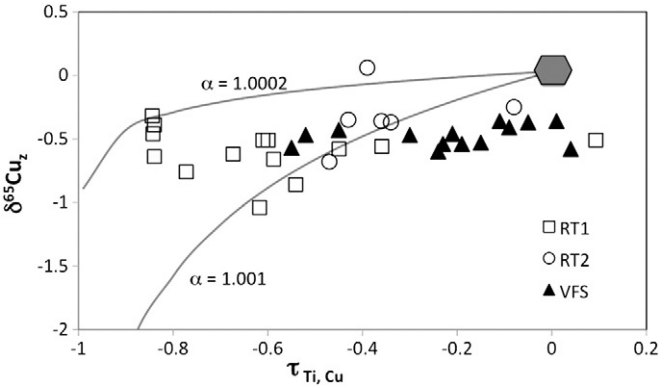

Fig. 5. Rayleigh model values plotted against observed soil values. The two curves represent hypothetical fractionation factors (between pore water and residue soil) of 1.0002 and 1.001, respectively. The grey pentagon represents Marcellus parent rock where conversion to soils starts.

It is interesting to note that the profiles mimic the patterns seen in leach cap Fe-oxides of the American Southwest and Iran (Mathur et al., 2010; Mirnejad et al., 2010) which have been interpreted to result also from oxidation of Cu-rich minerals. Specifically, in such deposits, hypogene minerals, generally found at depth, have been weathered to form supergene minerals under conditions of a lowering water table. In that case, Cu is leached from the oxidized zone (the leach cap) and re-precipitated at depth. The difference in Cu isotopic signature between the starting parent material (most hypogene sulfides show values = 0‰) and the residual Cu in the leach cap (<0‰) is on the order of several ‰. Most researchers argue that this difference is due to multiple episodes of leaching and re-precipitation that causes the final fractionation to be high. Consistent with this, the variation between the starting Marcellus shale and the residual soils is lower, barely 1‰, as expected for a system where only one leaching episode has occurred instead of multiple leaching + precipitation episodes. Nonetheless, the signatures present in the Marcellus are attributed to weathering of Cu from a sulfide leaving depleted Cu isotopic signatures that are analogous to the depleted isotopic signatures found in leach cap minerals.

4.4. Rayleigh models of the Cu concentration and isotope data during weathering

We can use Rayleigh models to investigate the quantitative changes in Cu concentration and isotope compositions during weathering of the Marcellus shale. The model can be written as:

$$R_Z = R_P f^{(\alpha-1)} \tag{3}$$

Here f is the fraction of Cu that remains in the residual soil in any sampled layer and α is the fractionation factor between solution and solid that describes pedogenesis of that layer. At the ridgetop sites, three Cu reservoirs are identified: M_p, M_z, and M_q are the mass of Cu in the original layer of the parent rock, the mass in the equivalent layer of the residual material (soils), and the mass lost from the layer respectively. Mass balance for each individual layer can be written:

$$M_p = M_z + M_q \tag{4}$$

It can easily be shown that the following expression is true for any given layer of a depletion profile (Brimhall and Dietrich, 1987) :

$$f = \frac{M_Z}{M_P} = 1 + \tau \tag{5}$$

$\delta^{65}Cu_p$ and $\delta^{65}Cu_z$ correspond to the Cu isotope ratios in the parent rock and in the individual layer of the residual soils respectively. Recognizing that δ and R are related according to Eq. (2), and rearranging Eqs. (3)–(5) yields:

$$\delta^{65}Cu_Z = \left(\left(\frac{\delta^{65}Cu_P}{1000} + 1\right) \times \left(1 + \tau_{Ti,Cu}\right)^{\alpha-1} - 1\right) \times 1000 \tag{6}$$

The soil layers sampled from different depths of the ridgetop sites have been weathered to different extents and are here considered to represent points on a Rayleigh fractionation curve with different τ and f values. Hypothetical curves of Cu isotope fractionation were constructed using different α values and Eq. (6). To bracket the ridgetop data, α values range from 1.0002 to 1.001 (Fig. 5). For this case, the fractionation factor during chemical leaching of Cu ($\Delta^{65}Cu = \delta^{65}Cu_q - \delta^{65}Cu_z$) is between 0.2 and 1‰. To date no fractionation factors have been determined for leaching of black shales

or pyrite; however, the difference between the average porewater (1.14‰) and parent soil (−0.03‰) yields a fractionation factor of ~1‰.

This Rayleigh fractionation calculation is based on the assumption that 1) individual layers within the residual soil are well-mixed and homogeneous reservoirs for Cu isotopes throughout the entire duration of weathering, 2) there has been no significant atmospheric or sediment input of Cu into ridge top soil, and 3) Cu mobility is not controlled by processes other than the weathering described here.

Nearly all of the ridgetop soils plot within the range of positive fractionation factors used. To date the positive fractionation factors used have been related to abiotic processes associated with the oxidation of Cu-sulfides. Thus, the most likely explanation of the concentration and isotopic data in combination appears to be abiotic oxidative weathering.

When we plot the VFS data using the model, a majority of measured values from the valley fall outside of fractionation curves defined by ridge top data (Fig. 5). The most likely explanation for this discrepancy is that another reservoir, not included yet in Eq. (4), is needed for mass balance. For example, precipitation and/or adsorption of secondary Cu may have occurred in the downslope sites as described in previous sections. This is in agreement with the observation that VFS soils are less depleted in Cu than the ridge top soils, which is opposite what would be expected given that the soils at valley floor are generally older and more extensively weathered. Notably, if the fractionation factor between secondary Cu precipitates and the solution is the same as that describing the primary Cu-bearing mineral-solution fractionation, then valley floor data should fall within the broad arc of $\tau_{Cu,Ti}$ — isotope data defined by ridge top soils. Instead, as shown in Fig. 5, the VFS data reside outside the modeled curves whereas the RT does not. The cause could be explained by Cu loss without significant fractionation from the valley soils, perhaps as particulate transport instead of aqueous transport. Such particle loss could also explain why the valley floor soils deviate from the ridge top soils in Fig. 5, i.e., they are more Cu-enriched than RT soils but isotopically similar to RT soils.

Furthermore, the data points in Fig. 5 that lie outside of the shaded areas are from 40 cm or deeper, while the data points that lie inside the shaded areas are from 30 cm or shallower. This observation could be consistent with Cu being added to the VFS site either as solutes or particles from upslope. Downslope flow (interflow) along the bedrock–regolith interface or through disturbed and fractured rock beneath that interface may bring Cu to the valley soils. Such subsurface interflow also has been inferred for the Susquehanna Shale Hills Observatory based on many types of observations (Jin et al., 2011).

5. Conclusions

In summary, a Rayleigh geochemical model demonstrates that weathering of ridgetop soils produces predictable Cu isotopic ratios and concentrations in the soils and waters of a zeroth-order catchment overlying the Marcellus shale in Huntingdon County, PA. The residual Cu-leached soils are isotopically depleted in ^{65}Cu while porewaters are isotopically enriched. The signature of isotopically enriched Cu in porefluids is attributed largely to oxidative weathering of Cu-containing pyrite in the Marcellus. This oxidation may have released almost 100% of the Cu in pyrite near the interface of bedrock and soil (i.e., the point of auger refusal). In contrast to the ridgetop soils, valley floor soils also must have acquired copper through re-precipitation or most likely, downslope particle transport along the hillslope, carrying Cu from the ridgetop to the valley floor position. No evidence supports significant Cu biocycling, although we cannot disprove that this mechanism contributes to the *Cu isotopic observations*. Our approach clearly demonstrates how the copper isotopic compositions of soils, porewaters, and rocks provide a means to track the process of dissolution, migration and precipitation of metal during weathering. The isotopic analysis provides key insights into the geochemical reactions taking place that are consistent with the elemental and mineralogical data.

Acknowledgements

Financial support was provided by the National Science Foundation under Grant No. CHE-0431328 for the Penn State Center for Environmental Kinetics Analysis to SLB and under Grant No. EAR-0725019 to C. Duffy (Penn State) for the Susquehanna/Shale Hills Critical Zone Observatory (SSHCZO). Special thanks to T. White, H. Gong, L. Liermann, W. Castro, M. Baker, M. Dendas, and J. Ruiz for assistance in field and laboratory analyses. Logistical support and/or data were provided by the NSF-supported SSHCZO.

References

Amundson, R., 2004. Soil formation. Surface and Ground Water, Weathering, and Soils, 5. Elsevier, Oxford (1–35 pp.).
Anon., 1990. Heavy metals in soils.
Anderson, M.K., Rauland-Rasmussen, K., Hansen, K., Strobel, B., 2002. Distribution and fractionation of heavy metals in pairs of arable and afforested soils in Denmark. European Journal Soil Science 53 (3), 491–502.
Balistrieri, L.S., Borrok, D.M., Wanty, R.B., Ridley, W.I., 2008. Fractionation of Cu and Zn isotopes during adsorption onto amorphous Fe(III) oxyhydroxide: experimental mixing of acid rock drainage and ambient river water. Geochimica et Cosmochimica Acta 72 (2), 311–328.
Beznosikov, V.A., Lodygin, E.D., Kondratenok, B.M., 2007. Assessment of background concentrations of heavy metals in soils of the northeastern part of European Russia. Eurasian Soil Science 40 (9), 949–955.
Bigalke, M., Weyer, S., Wilcke, W., 2009. Stable copper isotopes: a novel tool to trace copper behavior in hydromorphic soils. Soil Science Society of America Journal 74 (1), 60–73.
Bigalke, M., Weyer, S., Kobza, J., Wilcke, W., 2010. Stable Cu and Zn isotope ratios as tracers of sources and transport of Cu and Zn in contaminated soil. Geochimica et Cosmochimica Acta 74 (23), 6801–6813.
Bigalke, M., Weyer, S., Wilcke, W., 2011. Stable Cu isotope fractionation in soils during oxic weathering and podzolization. Geochimica et Cosmochimica Acta 75 (11), 3119–3134.
Borrok, D.M., Nimick, D.A., Wanty, R.B., Ridley, W.I., 2008. Isotopic variations of dissolved copper and zinc in stream waters affected by historical mining. Geochimica et Cosmochimica Acta 72 (2), 329–344.
Brantley, S.L., White, A.F., 2009. Approaches to modeling weathered regolith. In: Oelkers, E., Schott, J. (Eds.), Thermodynamics and Kinetics of Water–Rock Interaction: Reviews in Mineralogy and Geochemistry, pp. 435–484.
Brantley, S.L., Goldhaber, M.B., Ragnarsdottir, K.V., 2007. Crossing disciplines and scales to understand the critical zone. Elements 3 (5), 307–314.
Brantley, S.L., Buss, H., Lebedeva, M., Fletcher, R.C., 2011. Investigating the Complex Interface where Bedrock transforms to Regolith. Elsevier, Oxford–New York–Beijing, International (III), International (III), pp. S12–S15.
Brimhall, G.H., Dietrich, W.E., 1987. Constitutive mass balance relations between chemical composition, volume, density, porosity, and strain in metasomatic hydrochemical systems: results on weathering and pedogenesis. Geochimica et Cosmochimica Acta 51 (3), 567–587.
Campbell, R.W., 1976. Guidelines for Investigating a Suspected Copper Problem. Victorian Department of Agriculture.
de Jonge, L.W., Kjaergaard, C., Moldrup, P., 2004. Vadose Zone Journal 3 (2).
Du Laing, G., Vanthuyne, D.R.J., Vandecasteele, B., Tack, F.M.G., Verloo, M.G., 2007. Influence of hydrological regime on pore water metal concentrations in a contaminated sediment-derived soil. Environmental Pollution 147 (3), 615–625 (1987).
Ehrlich, S., et al., 2004. Experimental study of the copper isotope fractionation between aqueous Cu (II) and covellite, CuS. Chemical Geology 209 (3–4), 259–269.
Faill, R.T., 1998a. A geologic history of the north-central Appalachians; Part 3, The Alleghany Orogeny. American Journal of Science 298 (2), 131–179.
Faill, R., 1998b. The Geology of Pennsylvania: Harrisburg, Pennsylvania Geologic Survey: 888.
Flores-Veles, L.M., Ducaroir, J., Jaunet, A.M., Robert, M., 1996. Study of the distribution of copper in an acid sandy vineyard soil by three methods. European Journal of Soil Science 47, 523–532.
Fornadel, A., Mathur, R., Brantley, S., 2008. Geochemical and physical analysis of soil developed on the Marcellus shale in central Pennsylvania. GSA, Abstracts with Programs 40 (2), 19.
Gimeno-Garcia, E., Andreu, V., Boluda, R., 1995. Distribution of heavy metals in rice farming soils. Archives of Environmental Contamination and Toxicology 29 (4), 476–483.
Grybos, M., Davranche, M., Gruau, G., Pettijean, P., 2007. Is trace metal release in wetland soils controlled by organic matter mobility or Feoxyhydroxides reduction? Journal Colloid Interface Science 314 (2), 490–501.

Jaffe, L.A., Peucker-Ehrenbrink, B., Petsch, S.T., 2002. Mobility of rhenium, platinum group elements and organic carbon during black shale weathering. Earth and Planetary Science Letters 198 (3–4), 339–353.
Jin, L., et al., 2010. Mineral weathering and elemental transport during hill slope evolution at the Susquehanna/Shale Hills Critical Zone Observatory. Geochimica et Cosmochimica Acta 74 (13), 3669–3691.
Jin, L., Andrews, D.M., Holmes, G.H., Lin, H., Brantley, S.L., 2011. Opening the "Black Box": water chemistry reveals hydrological controls on weathering in the Susquehanna Shale Hills Critical Zone Observatory. Vadose Zone Journal 10 (3), 928–942.
Kabata-Pendias, A., Pendias, H., 2001. Trace Elements in Soils and Plants. CRC Press, Boca Raton, FL.
Kaste, J.M., Heimsath, A.M., Bostick, B., 2007. Short-term soil mixing quantified with fallout radionuclides. Geology 35 (3), 243–246.
Keller, C., Domergue, F.-L., 1996. Soluble and particulate transfers of Cu, Cd, Al, Fe and some major elements in gravitational waters of a Podzol. Geoderma 71 (3–4), 263–274.
Kimball, B.E., et al., 2009. Copper isotope fractionation in acid mine drainage. Geochimica et Cosmochimica Acta 73 (5), 1247–1263.
Lash, G.G., Engelder, T., 2011. Thickness trends and sequence stratigraphy of the Middle Devonian Marcellus Formation, Appalachian Basin: implications for Acadian foreland basin evolution. AAPG Bulletin 95 (1), 61–103.
Li, W., Jackson, S.E., Pearson, N.J., Alard, O., Chappell, B.W., 2009. The Cu isotopic signature of granites from the Lachlan Fold Belt, SE Australia. Chemical Geology 258 (1–2), 38–49.
Liermann, L.J., et al., 2011. Extent and isotopic composition of Fe and Mo release from two Pennsylvania shales in the presence of organic ligands and bacteria. Chemical Geology 281 (3–4), 167–180.
Marechal, C., Albarede, F., 2002. Ion-exchange fractionation of copper and zinc isotopes. Geochimica et Cosmochimica Acta 66 (9), 1499–1509.
Marechal, C.N., Telouk, P., Albarede, F., 1999. Precise analysis of copper and zinc isotopic compositions by plasma-source mass spectrometry. Chemical Geology 156 (1–4), 251–273.
Markl, G., Lahaye, Y., Schwinn, G., 2006. Copper isotopes as monitors of redox processes in hydrothermal mineralization. Geochimica et Cosmochimica Acta 70 (16), 4215–4228.
Mathur, R., et al., 2005. Cu isotopic fractionation in the supergene environment with and without bacteria. Geochimica et Cosmochimica Acta 69 (22), 5233–5246.
Mathur, R., et al., 2009. Exploration potential of Cu isotope fractionation in porphyry copper deposits. Journal of Geochemical Exploration 102 (1), 1–6.
Mathur, R., Dendas, M., Titley, S., Phillips, A., 2010. Patterns in the copper isotope composition of minerals in porphyry copper deposits in Southwestern United States. Economic Geology 105 (8), 1457–1467.
McLennan, S.M., Taylor, S.R., Hemming, S.R., 2006. Composition, differentiation, and evolution of continental crust; constraints from sedimentary rocks and heat flow. Evolution and Differentiation of the Continental Crust. Cambridge University Press, New York, NY. (92–134 pp.).
Minasny, B., McBratney, A.B., Salvador-Blanes, S., 2008. Quantitative models for pedogenesis; a review. Geoderma 144 (1–2), 140–157.
Mirnejad, H., Mathur, R., Einali, M., Dendas, M., Alirezaei, S., 2010. A comparative copper isotope study of porphyry copper deposits in Iran. Geochemistry - Exploration, Environment, Analysis 10 (4), 413–418.
Moore, D.M., Reynolds Jr., R.C., 1997. X-Ray Diffraction and the Identification and Analysis of Clay Minerals (2nd ed.). Oxford Univ. Press, New York.
Neaman, A., Chorover, J., Brantley, S.L., 2005a. Element mobility patterns record organic ligands in soils on early Earth. Geology 33 (2), 117–120.
Neaman, A., Chorover, J., Brantley, S.L., 2005b. Implications of the evolution of organic acid moieties for basalt weathering over geological time. American Journal of Science 305, 147–185.
Nordstrom, D.K., 1982. Aqueous pyrite oxidation and the consequent formation of secondary iron minerals. In: Kral, M. (Ed.), Acid Sulfate Weathering. Soil Science Society of America Special Publication. Soil Science Society of America, Madison, WI, pp. 37–56.
Obermajer, M., Fowler, M.G., Goodarzi, F., Snowdon, L.R., 1997. Organic petrology and organic geochemistry of Devonian black shales in southwestern Ontario, Canada. Organic Geochemistry 26 (3–4), 229–246.
Ollier, C., Pain, C., 1996. Regolith, Soils and Landforms. John Wiley and Sons, Chichester.
Palacios, C., Rouxel, O., Reich, M., Cameron, E., Leybourne, M., 2011. Pleistocene recycling of copper at a porphyry system, Atacama Desert, Chile: Cu isotope evidence. Mineralium Deposita 46 (1), 1–7.
Petsch, S.T., Berner, R.A., Eglinton, T.I., 2000. A field study of the chemical weathering of ancient sedimentary organic matter. Organic Geochemistry 31 (5), 475–487.
Pietrzak, U., McPhail, D.C., 2004. Copper accumulation, distribution, and fractionation in vineyard soils of Victoria, Australia. Geoderma 122 (3–4), 151–166.
Pokrovsky, O.S., Viers, J., Emnova, E.E., Kompantseva, E.I., Freydier, R., 2008. Copper isotope fractionation during its interaction with soil and aquatic microorganisms and metal oxy(hydr)oxides; possible structural control. Geochimica et Cosmochimica Acta 72 (7), 1742–1757.
Prasad, B.R., Basavaiah, S., Subba Rao, S., Subba Rao, I.V., 1984. Forms of copper in soils of grape orchards. Journal of the Indian Society of Soil Science 32 (2), 318–322.
Sageman, B.B., et al., 2003. A tale of shales; the relative roles of production, decomposition, and dilution in the accumulation of organic-rich strata, Middle-Upper Devonian, Appalachian Basin. Chemical Geology 195 (1–4), 229–273.
Soeder, D.J., 2010. The Marcellus Shale; resources and reservations. Eos, Transactions, American Geophysical Union 91 (32), 277–278.
Taylor, S.R., McLennan, S.M., 1985. The Continental Crust: Its Composition and Evolution. Blackwell, Oxford.
Taylor, G., McNally, G.H., 2001. Regolith; its history and environmental importance with particular reference to some engineering examples. Special Publication - Geological Society of Australia 21, 13–25.
Tiller, K.G., Merry, R.H., 1981. Copper pollution of agricultural soils. In: Longeragan, J.F., Robson, A.D., Graham, R.D. (Eds.), Proceedings of the Golden Jubilee International Symposium on Copper in Soils and Plants: Academic Press (Sydney), pp. 119–137.
Tuttle, M.L.W., Breit, G.N., 2009. Weathering of the New Albany Shale, Kentucky, USA: I. Weathering zones defined by mineralogy and major-element composition. Applied Geochemistry 24 (8), 1549–1564.
Tuttle, M.L.W., Breit, G.N., Goldhaber, M.B., 2009. Weathering of the New Albany Shale, Kentucky: II. Redistribution of minor and trace elements. Applied Geochemistry 24 (8), 1565–1578.
Vance, D., et al., 2008. The copper isotope geochemistry of rivers and the oceans. Earth and Planetary Science Letters 274 (1–2), 204–213.
Wilcke, W., Mosbach, J., Kobza, J., Zech, W., 1998. Distribution of Al and heavy metals in bulk soil and aggregates at three sites contaminated by the emissions of a Central Slovak Al Smelter. Water, Air, and Soil Pollution 106 (3–4), 389–402.
Wilcke, W.J., Krauss, M., Kobza, J., 2005. Concentrations and forms of heavy metals in Slovak soils. Journal of Plant Nutrition and Soil Science 168 (5), 676–686.
Wall, A.J., et al., 2011. A flow-through reaction cell that couples time-resolved X-ray diffraction with stable isotope analysis. Journal of Applied Crystallography 44 (2), 429–432.
Weber, F.-A., Voegelin, A., Kretzschmar, R., 2009. Multi-metal contaminant dynamics in temporarily flooded soil under sulfate limitation. Geochimica et Cosmochimica Acta 73 (19), 5513–5527.
Weinstein, C., et al., 2011. Isotopic fractionation of Cu in plants. Chemical Geology 286 (3–4), 266–271.
Zhu, X.K., et al., 2002. Mass fractionation processes of transition metal isotopes. Earth and Planetary Science Letters 200 (1–2), 47–62.